Conformal invariance in two-dimensional turbulence

D. BERNARD[1], G. BOFFETTA[2], A. CELANI[3] AND G. FALKOVICH[4]*

[1] Service de Physique Théorique de Saclay, CEA/CNRS, Orme des Merisiers, 91191 Gif-sur-Yvette Cedex, France
[2] Dipartimento di Fisica Generale and INFN, Università di Torino, via Pietro Giuria 1, 10125 Torino, Italy
[3] CNRS, INLN, 1361 Route des Lucioles, 06560 Valbonne Sophia Antipolis, France
[4] Physics of Complex Systems, Weizmann Institute of Science, Rehovot 76100, Israel
*e-mail: gregory.falkovich@weizmann.ac.il

The simplicity of fundamental physical laws manifests itself in fundamental symmetries. Although systems with an infinite number of strongly interacting degrees of freedom (in particle physics and critical phenomena) are hard to describe, they often demonstrate symmetries, in particular scale invariance. In two dimensions (2D) locality often extends scale invariance to a wider class of conformal transformations that allow non-uniform rescaling. Conformal invariance enables a thorough classification of universality classes of critical phenomena in 2D. Is there conformal invariance in 2D turbulence, a paradigmatic example of a strongly interacting non-equilibrium system? Here, we show numerically that some features of a 2D inverse turbulent cascade show conformal invariance. We observe that the statistics of vorticity clusters are remarkably close to that of critical percolation, one of the simplest universality classes of critical phenomena. These results represent a key step in the unification of 2D physics within the framework of conformal symmetry.

We consider here 2D incompressible turbulent motion of a fluid, which represents an appropriate description of large-scale motions of the atmosphere, and can also be realized in different laboratory settings[1–5]. As predicted[1], stirring at some forcing length scale L_f results in two turbulence cascades, with the formation of fine-scale vortical structures and large-scale velocity structures. In 2D, squared vorticity $\omega^2 = (\nabla \times \boldsymbol{v})^2$ performs a direct cascade to small scales whereas kinetic energy $(1/2)\boldsymbol{v}^2$ flows from L_f to large scales, opposite to the three-dimensional case ($\boldsymbol{v}$ being velocity). We focus here on the inverse cascade of energy for which, not surprisingly in view of the presence of a strong interaction, there is no exact analytic theory. Phenomenological dimensional arguments give consistent predictions, although in two seemingly unrelated ways. Consider the velocity difference v_r at the distance r. On the one hand, it may be required that the kinetic energy v_r^2 divided by the typical time r/v_r must be constant and equal to the energy flux ϵ: $v_r^3 \sim \epsilon r$. On the other hand, it can be argued that vorticity, which cascades to small scales, must be in equipartition in the inverse cascade range[6]. If this is the case, the enstrophy $r^d \omega_r^2$ accumulated in a volume of size r is proportional to the typical time r/v_r at such a scale, that is, $r^d \omega_r^2 \sim r/v_r$, where d is the space dimensionality and ω_r is the vorticity coarse-grained over the scale r. Using $\omega_r \sim v_r/r$ we derive $v_r^3 \sim r^{3-d}$, which for $d = 2$ is exactly the requirement of constant energy flux. Amazingly, the requirements of vorticity equipartition (that is, equilibrium) and energy flux (that is, turbulence) give the same Kolmogorov–Kraichnan scaling in 2D. Experiments[4,5,7] and numerical simulations[8] indeed demonstrate scale-invariant statistics with the vorticity having scaling dimension 2/3: $\omega_r \propto r^{-2/3}$.

Our goal here is to find out whether scale invariance can be extended to conformal invariance at least for some properties of 2D turbulence. Under conformal transformations, the lengths are re-scaled non-uniformly yet the angles between vectors are left unchanged (a useful property in navigation cartography where it is often more important to aim in the right direction than to know the distance)[9,10]. The novelty of our approach is that we analyse the inverse cascade by describing the large-scale statistics of the boundaries of vorticity clusters, that is, large-scale zero-vorticity
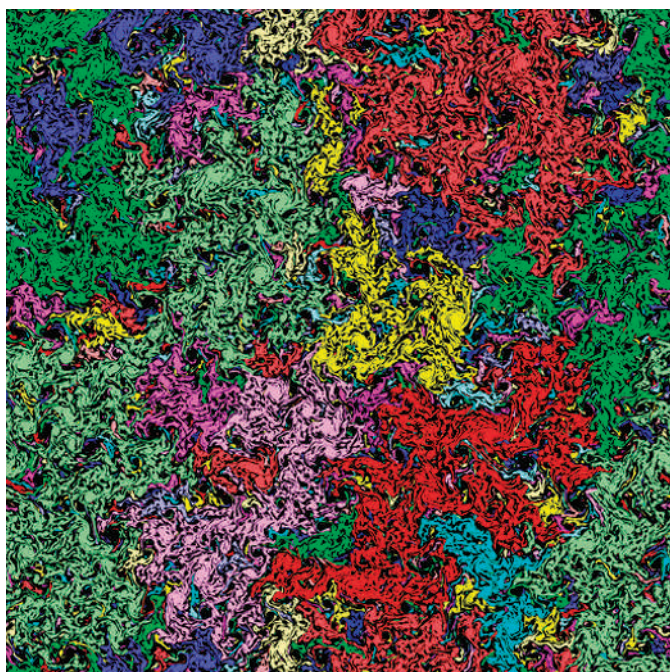
Figure 1 Vorticity clusters. These are defined as connected regions with the same sign of vorticity (here positive). Colours are arbitrarily attributed to different clusters. Regions of negative vorticity are black. L_f is one hundredth of the box side.
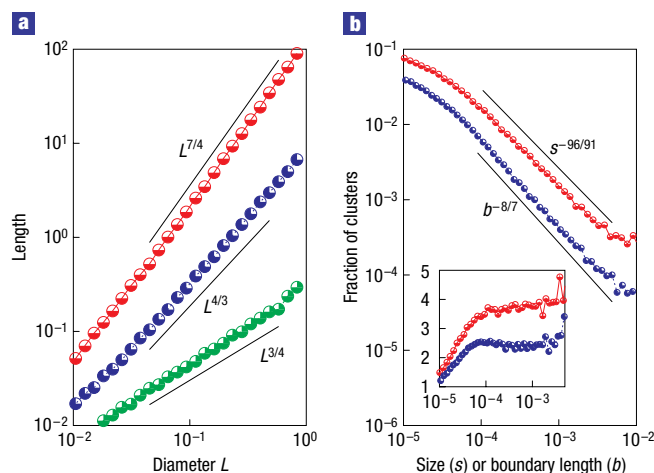

Figure 2 Fractal dimensions and probabilities of size and boundary length for vorticity clusters. a, The fractal dimensions are the slopes of the length–diameter dependencies in log–log coordinates for the boundary of filled clusters (red), for the outer boundary (blue) and for the necks of large fjords/peninsulae (green). The solid lines have slopes with the exact values for SLE_6 curves, $7/4$, $4/3$ and $3/4$, respectively. Fractal dimensions are obtained by computing the average length for a given diameter of the cluster. **b**, The fraction of clusters with sizes between s and $1.25s$ (red) and with boundary lengths between b and $1.25b$. The solid lines are the predictions from the percolation theory. Inset: The same data multiplied by $s^{96/91}$ and $b^{8/7}$, respectively. The vertical scale is linear to appreciate the plateau in the compensated plot.

lines. In equilibrium critical phenomena, cluster boundaries in the continuous limit of vanishingly small lattice size were found to belong to a remarkable class of curves that can be mapped into a brownian walk (called stochastic Loewner evolution or SLE curves)[11–19]. Namely, consider a curve $\gamma(t)$, where t is time, that starts at a point on the boundary of the half-plane H (by conformal invariance any planar domain is equivalent to the upper half-plane). One can map the half-plane H minus the curve $\gamma(t)$ back onto H by an analytic function $g_t(z)$, which is unique on imposing the condition $g_t(z) \sim z + 2t/z + O(1/z^2)$ at infinity. The growing tip of the curve is mapped into a real function $\xi(t)$. In 1923 it was found[20] that the conformal map $g_t(z)$ and the curve $\gamma(t)$ are fully parametrized by the driving function $\xi(t)$. Almost 80 years later, random curves were considered[11] in planar domains and it was shown that their statistics are conformally invariant if $\xi(t)$ is a brownian walk, that is, its increments are identically and independently distributed and $\langle(\xi(t)-\xi(0))^2\rangle = \kappa t$, where κ is the diffusivity. In simple words, the locality in time of the brownian walk translates into the local scale invariance of SLE curves, that is, conformal invariance. SLE_κ provides a natural classification (by the value of κ) of boundaries of clusters of 2D critical phenomena[16] described by conformal field theories (CFT)[10,21] and allows many results to be established (see refs 16–19 for a review).

The fractal dimension of SLE_κ curves is known to be[22,23] $D_\kappa = 1 + \kappa/8$ for $\kappa < 8$. To establish a possible link, let us try to relate the Kolmogorov–Kraichnan phenomenology to the fractal dimension of the boundaries of vorticity clusters. Note that it should be distinguished between the dimensionality two of the full vorticity-level set (which is space-filling) and a single zero-vorticity line that encloses a large-scale cluster[24]. Consider the vorticity cluster of gyration radius L that has the 'outer boundary' of perimeter P (that boundary is the part of the zero-vorticity line accessible from outside, see Fig. 3 for an illustration). The

vorticity flux through the cluster, $\int \omega dS \sim \omega_L L^2$, must be equal to the velocity circulation along the boundary, $\Gamma = \oint \boldsymbol{v} \cdot d\boldsymbol{\ell}$, where dS and $d\boldsymbol{\ell}$ are respectively differentials of contour area and length. The Kolmogorov–Kraichnan scaling is $\omega_L \sim \epsilon^{1/3} L^{-2/3}$ (coarse-grained vorticity decreases with scale because contributions with opposite signs partially cancel) so that the flux is proportional to $L^{4/3}$. As for circulation, as the boundary turns every time it meets a vortex, such a contour is irregular on scales larger than the pumping scale. Therefore, only the velocity at L_f is expected to contribute to the circulation; such a velocity can be estimated as $(\epsilon L_f)^{1/3}$ and it is independent of L. Hence, circulation should be proportional to the perimeter, $\Gamma \propto P$, which gives $P \propto L^{4/3}$, that is, the fractal dimension of the exterior of the vorticity cluster is expected to be $4/3$.

Let us check this hypothesis by data analysis. A powerful tool for the study of 2D turbulence is the numerical integration of the incompressible Navier–Stokes equations in a planar domain. By this method it is possible to achieve a range of dynamical length scales of about 10^4, whereas current laboratory experiments are limited to a scale separation of about 100. We present here the analysis of very-high-resolution numerical simulations (with up to $16{,}384^2$ grid points) of 2D inverse cascade (see Table 1 for the details). Vorticity clusters are shown in Fig. 1. We denote D_* the fractal dimension of their exterior boundary (without self-intersections). As shown in Fig. 2a, D_* is indeed close to $4/3$. Moreover, the fractal dimension of the boundary itself is close to $D = 7/4$. Of course, having some particular dimension does not by itself imply that the curve belongs to SLE. Note, however, that the exterior perimeter of SLE_κ with $\kappa > 4$ is conjectured[25] to look locally as a SLE_{κ_*} curve with $\kappa_* = 16/\kappa < 4$ resulting in the duality relation $(D-1)(D_*-1) = 1/4$, as observed in our turbulence data. Moreover, $D_* = 4/3$ corresponds to a $SLE_{8/3}$ curve, which represents the continuum limit of a self-avoiding random walk, whereas the dual SLE_6 curve corresponds to a cluster boundary in
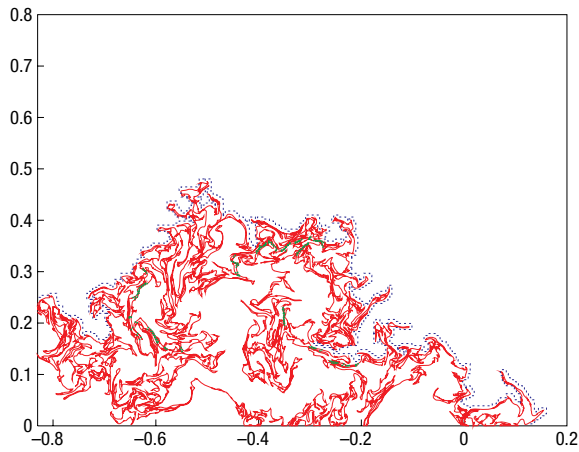
Figure 3 A portion of a candidate SLE trace obtained from the vorticity field. The red curve is a zero-vorticity line in the upper half-plane. The dashed blue line is the 'outer boundary' of the red curve, that is, the boundary of the region that can be reached from infinity without getting closer than L_f to the red curve. The green dots mark the necks of large fjords and peninsulae.

critical percolation. That prompts us to compare the probability distributions of sizes and boundary lengths between vorticity and percolation clusters. The size s of a cluster is the number of connected sites with the same sign of vorticity, the boundary length b is the number of sites that belong to the cluster but are adjacent to sites of different sign and the gyration radius L is the side of the smallest square that covers the cluster. The results shown in Fig. 2b are in a good agreement with the exact results from percolation theory.

The two SLEs with $\kappa = 6$ and $\kappa_* = 8/3$ correspond to CFT with zero central charge, which means that the scale invariance remains unbroken even when the system is on a manifold with corners or with a non-zero Euler number (a topological invariant determined by the number of handles and boundaries). Also, SLE_6 curves are singled out by a 'locality property' (the curve does not feel the boundary until it touches it), whereas their dual $SLE_{8/3}$ has the 'restriction property' (the statistics of the curves conditioned not to visit some region are the same as in the domain without this region)[12–16]. How does all this relate to 2D turbulence?

Now we show by a straightforward check that, within statistical accuracy, large-scale zero-vorticity lines are indeed SLE curves, that is they are conformally invariant and possess remarkable properties of a kind that has never been studied in turbulence. Zero-vorticity isolines that are candidate SLE traces are identified as follows. First, a horizontal line representing the real axis in the complex plane is drawn across the vorticity field. Second, an explorer starting from the origin at the real axis walks on the zero-vorticity isoline

keeping the positive vorticity sites always on the right. Third, when the explorer hits the real axis it treads on it, always leaving the positive region on its right-hand side until it can re-enter the upper half-plane. This eventually leads the explorer to infinity in an unbounded domain. An example of the outcome of this search is shown in Fig. 3. Strictly speaking, this procedure faithfully reproduces all the details of the statistics only if there is a locality property (meaning that the exploration process does not feel the boundary before it hits it), which holds for SLE_6. As we obtain as a result SLE with $\kappa \approx 6$, our procedure is self-consistent; we also checked that shifting and turning the line does not modify the results presented below. To determine which driving function $\xi(t)$ can generate such a curve, one needs to find the sequence of conformal maps $g_t(z)$ that map the half-plane H minus the curve into H itself. We approximate $g_t(z)$ by a composition of discrete, conformal slit maps that swallow one segment of the curve at a time (a slight variation of the techniques presented in http://www.math.washington.edu/~marshall/preprints/zipper.pdf). This results in a sequence of 'times' t_i and driving values ξ_i that approximate the true driving functions. If the zero-vorticity isolines in the half-plane are actually SLE traces, then the driving function should behave as an effective diffusion process at sufficiently large times. We have collected 1,607 putative traces. The data presented by blue triangles in Fig. 4 show that the ensemble average $\langle \xi(t)^2 \rangle$ indeed grows linearly in time: the diffusion coefficient κ is very close to the value 6, with an accuracy of 5% (see inset). The average $\langle \xi(t) \rangle$ vanishes by the reflection symmetry of the Navier–Stokes equations. In addition, the probability distribution functions of $\xi(t)/(\kappa t)^{1/2}$ collapse onto a standard gaussian distribution at all times t. Therefore, we expect that $\xi(t)$ tend to a true brownian motion and zero-vorticity lines to become SLE_κ traces with κ very close to 6 in the limit of vanishingly small L_f. To appreciate how remarkable this property is, pink symbols in the lower inset in Fig. 4 show for comparison the results of the same procedure for the isolines of a gaussian field having the same Fourier spectrum as vorticity but randomized phases. The slow incomplete recovery to $\kappa = 6$ for the random-phase field occurs at the scales where the power-law correlation is already cut off by friction and the field becomes truly uncorrelated.

The identification of isovorticity lines as SLE_κ curves allows powerful techniques borrowed from the theory of stochastic differential equations and conformal mapping theory to be applied, and analytic predictions to be obtained for some non-trivial statistical properties of vorticity clusters. The first example is the probability that a point $z = \rho e^{i\theta}$, where θ is the angle between the point and the origin, and ρ is the distance from the origin, inside the upper half-plane is surrounded by a positive vorticity cluster connected to the positive real axis. In this event, it is not possible to reach infinity with a continuous path starting at z without treading on positive vorticity sites. For this to happen, the zero-vorticity line must leave the point z on its right. The probability of such an event depends only on the angle θ and it assumes a particularly simple form in terms of hypergeometric functions[26]. In the inset of Fig. 5

Table 1 Parameters of the simulations. N spatial resolution, dx grid spacing, ν viscosity, α friction, $u_{r.m.s.}$ root-mean-square velocity, L_f forcing length scale, $\ell_d = \nu^{1/2}/\eta_\nu^{1/6}$ enstrophy dissipative scale, ε_I energy injection rate, ε_ν viscous energy dissipation rate, ε_α energy dissipation by large-scale friction (energy growth rate for $N = 16,384$), η_I enstrophy injection rate, η_ν viscous enstrophy dissipation rate, η_α enstrophy dissipation by friction (enstrophy growth rate for $N = 16,384$).

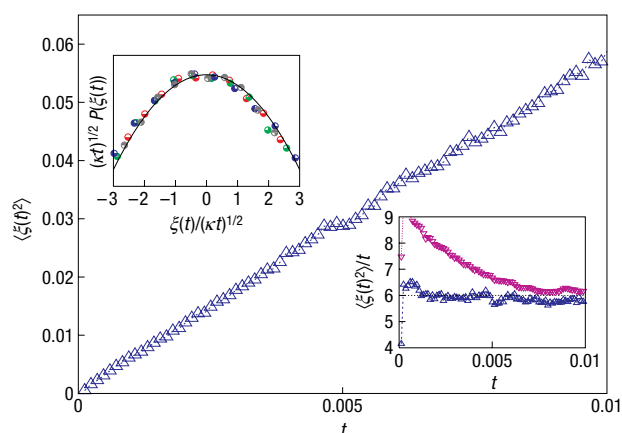| N	dx	ν	α	$u_{r.m.s.}$	L_f	ℓ_d	ε_I	ε_ν	ε_α	η_I	η_ν	η_α
2,048	4.9×10^{-4}	2×10^{-5}	0.015	0.26	0.01	2.4×10^{-3}	3.9×10^{-3}	1.8×10^{-3}	2.1×10^{-3}	39.3	38.0	1.3
4,096	2.4×10^{-4}	5×10^{-6}	0.024	0.26	0.01	1.2×10^{-3}	3.9×10^{-3}	0.7×10^{-3}	3.2×10^{-3}	39.3	36.1	3.2
8,192	1.2×10^{-4}	2×10^{-6}	0.025	0.27	0.01	7.8×10^{-4}	3.9×10^{-3}	0.3×10^{-3}	3.6×10^{-3}	39.3	35.3	4.0
16,384	0.6×10^{-4}	1×10^{-6}	0.0	0.24	0.01	5.5×10^{-4}	3.8×10^{-3}	0.2×10^{-3}	3.6×10^{-3}	39.5	37.6	1.9

Figure 4 The driving function is an effective diffusion process with diffusion coefficient $\kappa = 6 \pm 0.3$. The inverse cascade range corresponds to $5 \times 10^{-5} < t < 10^{-2}$. Main frame: the linear behaviour of $\langle \xi(t)^2 \rangle$. Lower-right inset: Diffusivity, blue for vorticity isolines, pink for the field with randomized phases. Upper-left inset: The probability density function of the rescaled driving function $\xi(t)/(\kappa t)^{1/2}$ at four different times $t = 0.0012$ (blue), 0.003 (green), 0.006 (red), 0.009 (grey); the solid line is the gaussian distribution $g(x) = (2\pi)^{-1/2} \exp(-x^2/2)$.

we show that the analytic solution fits very well the numerical data with $\kappa = 5.9$. The second example is the probability that a vorticity cluster spans the rectangle joining two opposite sides. What is the average number of such spanning clusters? What is the probability that a 'four-legged cluster' joins all four sides? By scale invariance these quantities depend only on the aspect ratio r of the rectangle, and their precise dependence can be found by exploiting conformal invariance. In the context of critical percolation, formulae for such probabilities have been derived[27,28] and later proven[29,30]. In the main frame of Fig. 5 we show that numerical data for vorticity clusters follow very closely the expectations for SLE$_6$. We have also checked (green symbols in Fig. 2) that the set of narrow necks that enclose large fjords or large peninsulae has dimension[31] 3/4 (the set is defined by the pairs of points on the curve that are closer than L_f yet separated by an arclength larger than $1,000 L_f$). This all gives further support to the result that zero-vorticity lines are conformal invariant and belong to the same class of universality as boundaries of percolation clusters.

Whether the statistics of the zero-vorticity isolines indeed fall into the simplest universality class of critical phenomena (and the fractal dimensions are exactly 7/4 and 4/3) deserves to be a subject of more study. Do our findings signify that the universal nature of percolation extends to turbulence as well as to diffusion-limited aggregation[32] and quantum chaos[33]? At the present level it has the status of a tantalizing conjecture with strong—although not conclusive—support from the data. In view of the non-local constraint imposed by the flow incompressibility, it is surprising that the statistics of zero-vorticity isolines (within experimental accuracy) enjoy the locality property inherited by their SLE$_6$ nature. Recall that continuous percolation can be constructed as a 'flooded landscape' determined by some short-correlated random height function. However, the vorticity field in the inverse cascade is not short-correlated; it has power-law correlation $\langle \omega(0) \omega(\mathbf{r}) \rangle \propto r^{-4/3}$. When the pair correlation function falls slower than $r^{-3/2}$ then the system is not expected generally to belong to the universality class of uncorrelated percolation and to be conformal invariant[34]. Indeed, we have seen that the field having the same pair correlation function as the vorticity yet randomized phases of the Fourier harmonics
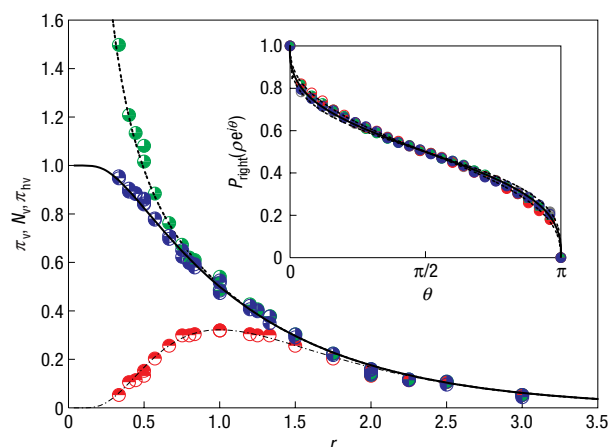

Figure 5 Crossing and surrounding probability for vorticity clusters. Main frame: the probability π_v that a cluster crosses from top to bottom a rectangle of aspect ratio r (blue), the average number N_v of vertically crossing clusters (green) and the probability π_{hv} of a 'four-legged' cluster joining all sides of the rectangle (red). The lines are the exact results for $\kappa = 6$:
$\pi_v = (3\Gamma(2/3)/\Gamma(1/3)^2)\eta^{1/3} \, _2F_1((1/3),(2/3);(4/3);\eta)$ with $\eta = [(1-k)/(1+k)]^2$ and $r = K(1-k^2)/[2K(k^2)]$ (Cardy–Smirnov, thick solid line); $N_v = (1/2)[\pi_v + \pi_{hv} - (\sqrt{3}/2\pi)\log\eta]$ (Cardy, thick dashed line); $\pi_{hv} = \pi_v - (\eta/\Gamma(2/3)\Gamma(1/3)) \, _3F_2(1,1,(4/3);2,(5/3);\eta)$ (Watts–Dubédat, thin dotted line). $_2F_1$ and $_3F_2$ are confluent hypergeometric functions. Inset: the probability that a zero-vorticity line in the upper half-plane leaves the point $\rho e^{i\theta}$ to its right, for $\rho = 0.048, 0.064, 0.080, 0.096$. The prediction for SLE$_\kappa$ traces is $P = (1/2) + (\Gamma(4/\kappa)/\sqrt{\pi}\Gamma((8-\kappa)/2\kappa)) \, _2F_1((1/2),(4/\kappa);(3/2);-\cot^2\theta)\cot\theta$, shown as a thick solid line for $\kappa = 5.9$ (the best fit). The dashed lines are the probabilities for $\kappa = 5.7$ (upper) and $\kappa = 6.1$ (lower).

does not have conformal invariant isolines (pink symbols in the lower inset in Fig. 4). We thus conclude that there is indeed something special about the vorticity (which has non-trivial phase correlations and higher moments) produced by 2D turbulence. It is also intriguing to notice that conformal field theory of critical percolation possesses a field of scaling dimension 2/3, identical to the one for the vorticity in Kolmogorov–Kraichnan phenomenology. We may also wonder how conformal invariance is broken in statistical properties of non-zero vorticity isolines. Let us stress that we have found conformal invariance for zero-vorticity isolines, but not yet for correlation functions as expected[3]; in the related problem of a passive scalar in turbulent flow, the correlation functions are not conformal invariant[6,35].

We have developed a numerical tool for testing conformal invariance in physical systems, established this symmetry (within experimental accuracy) for 2D inverse cascade and used it as a powerful tool in turbulence study, which allowed us to make quantitative predictions confirmed by the experiment. This shows how conformal invariance spans the whole range of physics, from exalted subjects such as string theory and quantum gravity, through statistical mechanics and condensed matter, down to earthly atmospheric turbulence.

References

1. Kraichnan, R. H. Inertial ranges in two-dimensional turbulence. *Phys. Fluids* **10,** 1417–1423 (1967).
2. Kraichnan, R. H. & Montgomery, D. Two-dimensional turbulence. *Rep. Prog. Phys.* **43,** 547–619 (1980).
3. Polyakov, A. M. The theory of turbulence in two dimensions. *Nucl. Phys. B* **396,** 367–385 (1993).
4. Tabeling, P. Two-dimensional turbulence: a physicist approach. *Phys. Rep.* **362,** 1–62 (2002).

5. Kellay, H. & Goldburg, W. I. Two-dimensional turbulence: a review of some recent experiments. *Rep. Prog. Phys.* **65,** 845–894 (2002).

6. Falkovich, G., Gawedzki, K. & Vergassola, M. Particles and fields in fluid turbulence. *Rev. Mod. Phys.* **73,** 913–975 (2001).

7. Chen, S. *et al. 57th APS Meeting of the Division of Fluid Dynamics* (APS, Seattle, Washington, 2004).

8. Boffetta, G., Celani, A. & Vergassola, M. Inverse energy cascade in two-dimensional turbulence: Deviations from Gaussian behavior. *Phys. Rev. E* **61,** R29–R32 (2000).

9. Polyakov, A. M. Conformal symmetry of critical fluctuations. *JETP Lett.* **12,** 381–383 (1970).

10. Belavin, A. A., Polyakov, A. M. & Zamolodchikov, A. A. Conformal field theory. *Nucl. Phys. B* **241,** 333–380 (1984).

11. Schramm, O. Scaling limits of loop-erased random walks and uniform spanning trees. *Israel J. Math.* **118,** 221–288 (2000).

12. Lawler, G., Schramm, O. & Werner, W. Values of Brownian intersection exponents I: Half-plane exponents. *Acta Math.* **187,** 237–273 (2001).

13. Lawler, G., Schramm, O. & Werner, W. Values of Brownian intersection exponents II: Plane exponents. *Acta Math.* **187,** 275–308 (2001).

14. Lawler, G., Schramm, O. & Werner, W. Values of Brownian intersection exponents III: Two-sided exponents. *Ann. Inst. H. Poincare* **38,** 109–123 (2002).

15. Lawler, G., Schramm, O. & Werner, W. Conformal restriction properties. The chordal case. *J. Am. Math. Soc.* **16,** 915–955 (2003).

16. Lawler, G. Conformally invariant processes in the plane. *Math. Surveys Monogr.* **114,** 1–242 (2005).

17. Gruzberg, I. & Kadanoff, L. The Loewner equation: maps and shapes. *J. Stat. Phys.* **114,** 1183–1198 (2004).

18. Cardy, J. SLE for theoretical physicists. *Ann. Phys.* **318,** 81–118 (2005).

19. Bauer, M. & Bernard, D. in *Proc. NATO Advanced Study Institute on String, France, June 2004* (eds Baulieu, L., de Boer, J., Pioline, B. & Rabinovici, E.) (NATO Science Series, Vol. 208, Springer, Berlin, 2006).

20. Löwner, K. Untersuchungen über schlichte konforme Abbildungen des Einheitskreises. *Math. Ann.* **89,** 103–121 (1923).

21. Bauer, M. & Bernard, D. Conformal field theories of stochastic Loewner evolutions. *Commun. Math. Phys.* **239,** 493–521 (2003).

22. Saleur, H. & Duplantier, B. Exact determination of the percolation hull exponent in two dimensions. *Phys. Rev. Lett.* **58,** 2325–2328 (1987).

23. Beffara, V. The dimension of the SLE curves. Preprint at <http://arxiv.org/abs/math.PR/0211322> (2002).

24. Kondev, J. & Henley, C. L. Geometrical exponents of contour loops on random Gaussian surfaces. *Phys. Rev. Lett.* **74,** 4580–4583 (1995).

25. Duplantier, B. Conformally invariant fractals and potential theory. *Phys. Rev. Lett.* **84,** 1363–1367 (2000).

26. Schramm, O. A percolation formula. *Elect. Comm. Probab.* **6,** 115–120 (2001).

27. Cardy, J. Critical percolation in finite geometries. *J. Phys. A* **25,** L201–L206 (1992).

28. Watts, G. A crossing probability for percolation in two dimensions. *J. Phys. A* **29,** L363–L368 (1996).

29. Smirnov, S. Critical percolation in the plane: conformal invariance, Cardy's formula, scaling limits. *C.R. Acad. Sci. Paris I Math.* **333,** 239–244 (2001).

30. Dubédat, J. Excursion decompositions for SLE$_6$ and Watts' crossing formula. Preprint at <http://arxiv.org/abs/math.PR/0405074> (2004).

31. Nienhuis, B. Exact critical point and critical exponents of O(n) models in two dimensions. *Phys. Rev. Lett.* **49,** 1062–1065 (1982).

32. Meakin, P. & Family, F. Diverging length scales in diffusion-limited aggregation. *Phys. Rev. A* **34,** 2558–2560 (1986).

33. Bogomolny, E. & Schmit, C. Percolation model for nodal domains of chaotic wave functions. *Phys. Rev. Lett.* **88,** 114102 (2002).

34. Weinrib, A. Long-correlated percolation. *Phys. Rev. B* **29,** 387–395 (1984).

35. Falkovich, G. & Fouxon, A. Anomalous scaling of a passive scalar in turbulence and equilibrium. *Phys. Rev. Lett.* **94,** 214502 (2005).

Competing financial interests

The authors declare that they have no competing financial interests.